# Segregation of mass at the periphery of N-isopropylacrylamide-co-acrylic-acid microgels at high temperatures

John S. Hyatt, Changwoo Do, Xiaobo Hu, Hong Sung Choi, Jin Woong Kim, L. Andrew Lyon, and Alberto Fernandez-Nieves

Phys. Rev. E **92**, 030302 — Published 29 September 2015

DOI: 10.1103/PhysRevE.92.030302

# Segregation of Mass at the Periphery of NIPAM-*co*-AAc Microgels at High Temperatures

John S. Hyatt,[1] Changwoo Do,[2] Xiaobo Hu,[3] H. S. Choi,[4] J. W. Kim,[5,6] L. Andrew Lyon,[3] and Alberto Fernandez-Nieves[1]

[1]*School of Physics, Georgia Institute of Technology, Atlanta, GA 30332-0430, USA*
[2]*Biology and Soft Matter Division, Neutron Sciences Directorate, Oak Ridge National Laboratory, Oak Ridge, TN 37831, USA*
[3]*School of Chemistry & Biochemistry, Georgia Institute of Technology, Atlanta, GA, 30332, USA*
[4]*Shinsegae International, 422 Apgujeong-ro, Gangnam-gu, Seoul 135-954, South Korea*
[5]*Department of Applied Chemistry, Hanyang University, Ansan, Gyeonggi-do 426-791, South Korea*
[6]*Department of Bionano Technology, Hanyang University, Ansan, Gyeonggi-do 426-791, South Korea*

(Dated: August 18, 2015)

We investigate poly(*N*-isopropylacrylamide) (pNIPAM) microgels randomly copolymerized with large mol% of protonated acrylic acid (AAc), finding that above the lower critical solution temperature the presence of the acid strongly disrupts the pNIPAM's collapse, leading to unexpected new behavior at high temperatures. Specifically, we see a dramatic increase in the ratio $R_g/R_h$ above the theoretical value for homogeneous spheres, and a corresponding increase of the network length scale, which we attribute to the presence of a heterogeneous polymer distribution that forms due to frustration of the pNIPAM's coil-to-globule transition by the AAc. We analyze this phenomenon using a Debye-Bueche-like scattering contribution as opposed to the Lorentzian term often used, interpreting the results in terms of mass segregation at the particle periphery.

Microgels synthesized from poly(*N*-isopropylacrylamide) (pNIPAM) have been widely studied for their thermoresponsive properties in water. Depending on the solvent quality, which is a function of temperature due to pNIPAM having a lower critical solution temperature, and the amount of crosslinker included in the synthesis, these particles can exhibit structural features spanning the colloid-polymer spectrum, ranging from star-polymer-like under certain conditions (low temperature, low crosslinker concentration) to core-shell or even hard-sphere-like under others (high temperature, high crosslinker concentration). Core-shell morphologies in particular can arise from reaction kinetics during synthesis that promote the early consumption of crosslinker during the initial stages [1, 2], leading to a more compact core surrounded by a fuzzy shell; in the extreme case of very high crosslinker concentration, or when high temperatures cause the pNIPAM and water to phase separate, the particles can approximate hard spheres [3, 4]. Other morphologies are available as well, such as grafting a shell of pNIPAM onto a compositionally different core [5] or copolymerizing NIPAM with another monomer, which can lead to different single-particle phase behavior. However, all of these cases share two broad similarities: first, that the limiting behavior in the most-deswollen case is that of homogeneous spheres, and second, that the mesh size of the polymer network inside the particles decreases with particle size.

Using microgels composed of NIPAM copolymerized with acrylic acid (AAc) at pH 3, where the AAc is not ionized, we see radically different behavior not attributable to either the presence of crosslinker or the volume phase transition of pNIPAM alone. Specifically, we measure the radius of gyration, defined as the root mean square distance of a particle's components from its center of mass, and the hydrodynamic radius, which represents the overall particle size, and obtain the ratio $R_g/R_h$. Note that high and low $R_g/R_h$ values mean that the particle mass is concentrated far from or near to the center of mass, respectively. We obtain that $R_g/R_h$ is greater than the theoretical homogeneous sphere value of $\sqrt{3/5}$ at high temperatures, indicating that the mass inside the particles is concentrated at the particle periphery, rather than uniformly distributed throughout the particles. Additionally, we observe that the length scale associated with the particles' internal structure increases, rather than decreases, with increasing temperature. We interpret these results in terms of the effect of neutral AAc, which induces the formation of heterogeneous clumps of polymer and frustrates the pNIPAM's coil-to-globule transition for high enough AAc content.

Our p(NIPAM-*co*-AAc) microgels have 24 mol% AAc randomly copolymerized with the NIPAM, and are crosslinked with 3 mol% poly(ethylene glycol) diacrylate (pEG-d), $CH_2CH\ CO-(OCH_2CH_2)_n-O\ CO\ CH\ CH_2$, where $n \sim 10$–$11$ is the number of repeat units. We use 3D dynamic light scattering (3DDLS), static light scattering (SLS), and small-angle neutron scattering (SANS) to characterize the particles. All measurements are made at pH 3, well below the $pK_a$ of AAc, which is 4.4; therefore, the AAc is neutral and the particles are not charged.

In a 3DDLS experiment, we measure the normalized intensity cross-correlation function as a function of lag time, $g_I(\tau)$, of two separate scattering experiments [6]. This is related to the electric field cross-correlation function, $g_E(\tau)$, via the Siegert relation, $g_I(\tau) - 1 = \beta\,|g_E(\tau)|^2$, where $\beta$, the intercept, is a measure of the signal-to-noise ratio that for a 3D cross-correlation experiment cannot exceed 0.25. For a diffusive system of dilute particles, $g_E(\tau) = \exp(-Dq^2\tau)$, where $D$ is the

diffusion coefficient of the particles and $q = \frac{4\pi n}{\lambda_0}\sin(\theta/2)$ is the scattering wave vector, with $n$ the solvent index of refraction, $\lambda_0$ the wavelength of the scattered light in vacuum, and $\theta$ the scattering angle. From $D$ and the Stokes-Einstein relation [7], we obtain the hydrodynamic radius of the particles, $R_h = k_B T/6\pi\eta D$, where $k_B$ is the Boltzmann constant, $T$ is the temperature, and $\eta$ is the solvent viscosity. We see $R_h$ decreases with temperature, as shown by the closed symbols in Fig. 1, consistent with what is reported in the literature for pNIPAM microgels [8].

Using SLS, we also measure the radius of gyration, $R_g$, of the particles. The form factor of particles in a dilute system is proportional to the intensity. All particle form factors share the same dependence on $R_g$ at low $q$, which corresponds to large length scales, regardless of the detailed particle structure [7]: for $qR_g \lesssim 2.5$, the particle form factor follows the Guinier decay, $P(q) \sim \exp\left[-(qR_g)^2/3\right]$. By fitting the low-$q$ portion of $P(q)$ to this decay, as shown by the dotted lines in Fig. 2, we obtain values of $R_g$ that, similarly to $R_h$, decrease with increasing temperature, as shown in Fig. 1.

The ratio $R_g/R_h$ is a measure of the scattering length density inside the particle. However, given that we expect the NIPAM and AAc monomers to be roughly evenly distributed throughout the particle, and that they scatter visible light approximately the same, since their bulk refractive indices are similar ($\sim 1.52$ for NIPAM [9, 10] and $\sim 1.42$ for AAc [11]), this ratio can be interpreted as a measure of the mass distribution inside the particle. Hence, $R_g/R_h$ can be taken to correspond to the ratio of the root-mean-square distance of the particle components from its center of mass, and the overall size of the particle. For homogeneous spheres, $R_g/R_h = \sqrt{3/5}$. At low temperatures, our values of $R_g/R_h \lesssim \sqrt{3/5}$. Remarkably, at high temperatures, this ratio increases, to a maximum of about 1, as shown in the inset of Fig. 1. Note that $R_g/R_h \sim 1$ is the theoretical value expected if all the mass is concentrated in a thin shell at the particle surface; the ratio cannot exceed 1 unless $R_h$ is significantly smaller than the particle size, which is unlikely [12], especially when the particles are deswollen.

We also analyze the full form factor of our particles as measured by SLS and SANS, in addition to the analysis of the Guinier regime described above. All SANS measurements were conducted on the EQ-SANS instrument at the Spallation Neutron Source at Oak Ridge National Laboratory using sample-to-detector distances of 4 m and 2.5 m, and minimum wavelengths of 9.5 $\mathring{A}$ and 2.5 $\mathring{A}$, respectively. The measured scattering intensity was corrected for detector sensitivity and the background from the empty cell. To combine the SANS and SLS results, we vertically scale the SANS results to obtain the best fit of all the data to a polydisperse core-shell form factor [4] with a generalized network term:

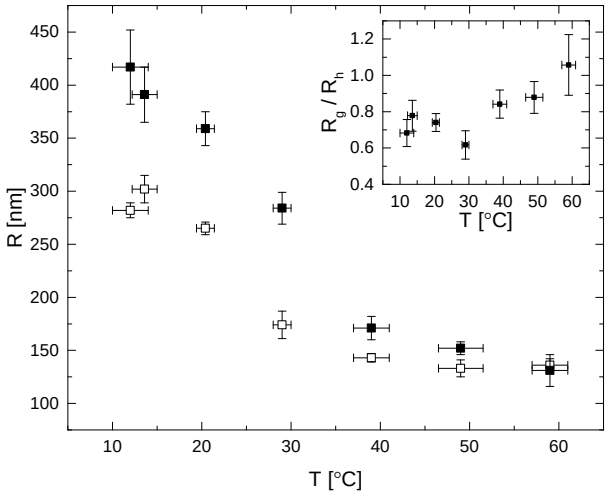


FIG. 1. Hydrodynamic radius (■) and radius of gyration (□) as a function of temperature measured using 3DDLS and SLS, respectively. The inset shows the resulting values of $R_g/R_h$ across the same temperature range.

$$P(q) = \frac{1}{\sqrt{2\pi}\sigma_p\langle R_c\rangle}\frac{1}{\langle V^2\rangle}\int \mathrm{d}R_c V(R_c,\sigma_s)^2 P_1(q,R_c) \times \exp\left[-\frac{1}{2}\left(\frac{R_c-\langle R_c\rangle}{\sigma_p\langle R_c\rangle}\right)^2\right] + I_1\frac{\Gamma(\mu)}{q\xi}\frac{\sin[\mu\arctan(q\xi)]}{[1+(q\xi)^2]^{\mu/2}} + I_0 \quad (1)$$

where the particle volume, $V(R_c,\sigma_s) = (4\pi/3)(R_c + 2\sigma_s)^3$, squared, divided by the mean squared-volume, $\langle V^2\rangle$, is included in the firs term of the equation to account for the fact the scattering length density of a particle is proportional to its volume squared. In addition,

$$P_1(q,R_c) = \left[3\frac{\sin(qR_c) - qR_c\cos(qR_c)}{(qR_c)^3}\exp\left(-\frac{(\sigma_s q)^2}{2}\right)\right]^2. \quad (2)$$

Eq. 2 is the monodisperse core-shell form factor obtained by convoluting the form factor of a hard sphere with radius $R_c$ with a Gaussian describing a fuzzy shell of total width $2\sigma_s$. The first term in Eq. 1 reflects polydispersity in the core size by taking an integral over a Gaussian distribution of core sizes with mean $\langle R_c\rangle$ and width $\sigma_p \cdot \langle R_c\rangle$. The second term in Eq. 1 is a network term as derived originally in the context of star polymers [13], with $\Gamma$ the gamma function, $\mu = D_f - 1$, with $D_f$ the polymer fractal dimension, and $\xi$ a length scale. This term reduces to the Lorentzian function $I_1/[1+(q\xi)^2]$, commonly used to describe polymer fluctuations in gels, in the limit $\mu \to 1$. In the limit $\mu \to 2$, however, it reduces to the Debye-Bueche scattering factor for inhomogeneous systems [14], $I_1/[1+(q\xi)^2]^2$. The last term in Eq. 1 is a constant term describing the scattering back-

ground. Note that inclusion of a prefactor in Eq. 1 does not change the fit, since in all conditions fitted $I_1 \ll 1$ and $I_0 \ll 1$. As a result, even without inclusion of this prefactor, this equation is, for all intents and purposes, normalized to 1.

We see good agreement between our data and Eq. 1. $\langle R_c \rangle$ and $2\sigma_s$ decrease with increasing temperature, consistent with the expected shrinking of the particle as temperature increases. Note that a fit with $\mu = 1$, corresponding to a Lorentzian, fails to match the SANS data at high temperatures, as shown in the inset in Fig. 2a. In contrast, at low temperatures, a fit with $\mu = 1$ reasonably describes the SANS data, shown with circles in Fig. 2b. However, there is no scaling that allows Eq. 1 with $\mu \sim 1$ to accurately reproduce the observed second minimum in the SLS form factor, shown with squares in Fig. 2b; only a comparatively sharp decay with $\mu \sim 2$ does that. Further, particularly at low temperature where the shell thickness is substantial, the asymptotic behavior of the first term in Eq. 1 is close to $q^{-6}$ due to the influence of the Gaussian convolution, and not to the $q^{-4}$ decay observed for Porod scattering from a sharp interface. As a result, the observed SANS decay cannot be explained as a remnant of the Porod scattering term. Thus, our data is better described in terms of the Debye-Bueche inhomogeneity term rather than the usual Lorentzian decay. Fitting parameters with $\mu = 2$ are listed in Table I.

We note that the combination of 3DDLS and SLS allows us to separate out only the single-scattering contribution to the measured intensity. This is necessary even for dilute systems of particles because at the minima of the form factor there is a disproportionately large contribution from multiple scattering, and as the SLS form factors in Fig. 2 show (squares), at low temperatures these minima are accessible. We correct for multiple scattering as usual for 3DDLS/SLS experiments [6], multiplying the measured intensity by $\sqrt{\beta/\beta_{ref}}$, where $\beta$ is the measured intercept and $\beta_{ref}$ is a reference intercept measured for an isotropic scatterer. SANS results are shown by circles in Fig. 2.

The increase of $R_g/R_h$ is unusual and very different to what is commonly observed for pNIPAM microgels crosslinked with bisacrylamide (BIS) and that have less AAc. As a result, we believe it is the presence of pEG-d, AAc, or both, that results in the observed high-temperature behavior. Previous work with pNIPAM microgels without AAc and crosslinked with 2 mol% pEG-d, with $n \sim 13$ repeat units per chain, also reported unusual, but different, behavior compared to what we observe [15]: in addition to the LCST deswelling around 32 °C, they observed a prior deswelling transition at 17.3 °C. Importantly, however, $R_g/R_h$ was always smaller or comparable to the homogeneous sphere value of $\sqrt{3/5}$. In addition, the form factor of these particles was fitted with a star polymer model with $\mu \sim 0.1$ at low temperatures, $\mu \sim 0.7$ near the LCST, and $\mu \sim 1$ at high temperatures. The internal structure of the particles at high temperature is thus well-described with a Lorentzian, in contrast to our experimental findings. Hence, it is unlikely that the high temperature behavior we observe in our microgels results from the presence of pEG-d.

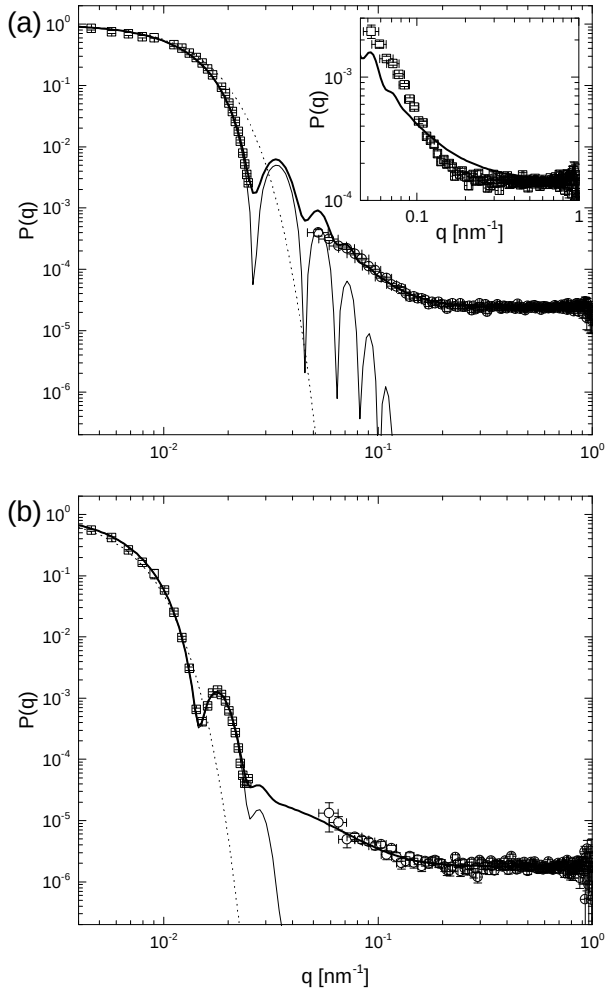


FIG. 2. Experimental form factors from SLS (□) and SANS (○), together with best fits to Eq. 1 (thick lines) and to just the first term in Eq. 1 (thin solid lines). (a) T = 49 °C, (b) T = 14 °C. Dotted lines show the Guinier fits to the low-$q$ SLS data. The inset in (a) shows a zoom of the SANS data together with the best fit to Eq. 1 using $\mu = 1$.

Alternatively, this behavior could result from the presence of large amounts of AAc. When charged, AAc causes swelling by drawing counterions from the outside solution into the particle. In contrast, neutral AAc exerts no influence on the swelling/deswelling behavior of the system beyond breaking up segments of pNIPAM, assuming it is randomly copolymerized throughout the particle, as in our case. To understand this, recall that the collapse of pNIPAM in water at its LCST is cooperative – that is, the entire pNIPAM chain collapses as a whole. The minimum chain length necessary for this collapse to occur is about 10 monomers long [16]. However, in the case of our particles, there is sufficient AAc to potentially frustrate this collapse. Indeed, previous

TABLE I. Parameters measured for the particles as a function of temperature. In all cases, $\mu = 2$. The uncertainty in fitting parameters of the SLS for measurements where a corresponding SANS measurement was made is smaller because those parameters were further constrained by the need to fit the SANS data. Otherwise, the polydispersity essentially represents an upper bound, as satisfactory fits could be made to the SLS data alone even with zero polydispersity.

| T [°C] | $\langle R_c \rangle$ [nm] | $2\sigma_s$ [nm] | $\sigma_p$ | $\xi$ [nm] |
|---|---|---|---|---|
| $12 \pm 2$ | $317 \pm 1$ | $136 \pm 4$ | $0.015 \pm 0.014$ | |
| $14 \pm 1$ | $306 \pm 2$ | $146 \pm 4$ | $0.048 \pm 0.01$ | $19 \pm 4$ |
| $20 \pm 1$ | $290 \pm 2$ | $121 \pm 8$ | $0.047 \pm 0.003$ | |
| $29 \pm 1$ | $210 \pm 1$ | $50 \pm 20$ | $0.015 \pm 0.014$ | |
| $39 \pm 2$ | $176 \pm 4$ | $30 \pm 30$ | $0.025 \pm 0.024$ | |
| $49 \pm 3$ | $170 \pm 3$ | $37 \pm 5$ | $0.075 \pm 0.007$ | $27.3 \pm 2.2$ |
| $59 \pm 2$ | $164 \pm 6$ | $59 \pm 5$ | $0.076 \pm 0.007$ | $30.2 \pm 2.5$ |

work [17] found that for randomly-copolymerized, neutral polymer chains comprised of NIPAM and AAc, an increasing fraction of chains failed to collapse above NIPAM's LCST as the AAc content increased. We thus hypothesize that it is the presence of neutral AAc in our particles which predominantly affects the high temperature behavior observed experimentally.

To test our hypothesis, we consider that the average number of monomers between crosslink points is $(73\% + 24\%)/3\% \sim 32$, and calculate the probability that there will be a run of 10 or more consecutive NIPAM monomers in a chain of 32 monomers, with a 75% probability that a given monomer is NIPAM and a 25% probability that it is AAc. We do so using that [18]

$$\mathcal{P}(\ell_n \geq m) = \sum_{j=1}^{\text{floor}[n/m]} (-1)^{j+1} \left[ p + \frac{n - jm + 1}{j}(1-p) \right] \times \binom{n-jm}{j-1} p^{jm} (1-p)^{j-1}, \tag{3}$$

where $\mathcal{P}(\ell_n \geq m)$ is the probability that there will be a run of successive "A" events with length $\ell_n$ greater than some number $m$, $p$ is the probability of an "A" event, and $1 - p$ is the probability of a "B" event. In this case, "A" represents a NIPAM monomer and "B" an AAc monomer, with $p = 0.75$, $m = 10$, and $n = 32$. We obtain that $\mathcal{P}(\ell_n \geq m) = 45\%$. Alternatively, we can use this value and solve for $m$. We obtain an average consecutive pNIPAM length and standard deviation of $m = 9 \pm 3$ monomers. Hence, we find there is about an even chance that a given polymer between two crosslinker points will have enough consecutive pNIPAM monomers to, at least, partially collapse. This implies that the microgel structure at the polymer level will be heterogeneous, since some monomer sequences will collapse and some will not, supporting the feasibility of our hypothesis.

Further confirmation comes from the fact that we observe that the network length scale, extracted from our SANS data, increases with increasing temperature (Table I). This is in contrast to previously reported values with pNIPAM/pEG-d microgels and no AAc, where the characteristic internal length scale, albeit one measured with a Lorentzian function, decreased with increasing temperature [15]. A similar trend has also been observed with pNIPAM microgels crosslinked with BIS [19]. Such a decrease indicates that the network length scale changes in an approximately affine way with the overall particle size. In our microgels, the characteristic internal length scale increases as the overall particle size shrinks. This, together with a uniform fitting parameter of $\mu = 2$, indicates the formation of relatively large heterogeneous clumps within the particle at high temperature, further emphasizing the key role played by the relatively large amount of neutral AAc in our particles. We do, however, emphasize that the clumps are not expected to be composed entirely of AAc; on the contrary, we expect that they would be formed from NIPAM-rich sequences that are able to collapse together, and are separated by regions of sequences comparatively rich in AAc that are therefore unable to collapse.

The observed increase in the heterogeneity length scale with temperature has an associated increase in $R_g/R_h$. In particular, while at low temperatures, the microgels display a core-shell mass distribution, as confirmed by the SLS form factors and an $R_g/R_h < \sqrt{3/5}$, at the highest temperatures, values of $R_g/R_h > \sqrt{3/5}$ indicate a morphology with clumps preferentially formed at the particle periphery rather than being concentrated at the center or distributed homogeneously throughout. Indeed, despite that this heteregenous clumping induced by the ability of AAc to frustrate pNIPAM-chain collapse is likely to occur throughout the particle, it will be more present in its periphery where there is less PEG-d; the crosslinker reacts faster than the monomers and thus it is expected that its concentration will decrease from the particle center towards the particle periphery. As a result, we expect the monomer chains will be shorter near the particle center, hence decreasing the chances of long-enough NIPAM sequences that could potentially collapse at high temperatures. At intermediate temperatures, $R_g/R_h \approx \sqrt{3/5}$. We schematically summarize the structural changes of our microgels with temperature in Fig. 3.

In conclusion, we have observed an increasing $R_g/R_h$

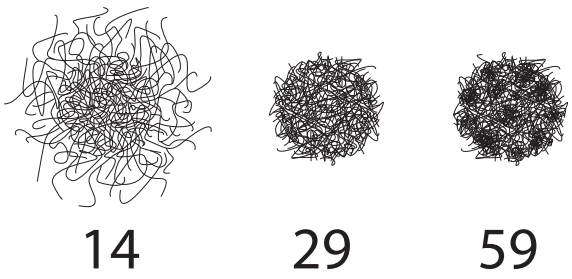


FIG. 3. Representative schematic of proposed microgel conformation changes as a function of temperature in °C. We emphasize that the heterogeneities in the schematic for 59 °C are not drawn to scale; the internal length scale $\xi$ is at least a factor of 10 smaller than the particle diameter. Hence, these heterogeneities are relevant at the polymer-level and do not singificantly affect the particle structure at larger length scales. This is why they are only apparent at the $q$-values probed with SANS.

with temperature that coincides with a similar increase in heterogeneity length scale $\xi$ as modeled with a Debye-Bueche scattering term, in measurements of NIPAM-*co*-AAc microgels with a high mol% of AAc. We attribute this to the frustration of the pNIPAM coil-to-globule transition caused by the presence of large amounts of neutral AAc, which interrupt the continuous chains of pNIPAM the transition requires. At high temperatures, the measured $R_g/R_h$ approaches 1, the theoretical maximum for a nondraining system, well above the usual homogeneous sphere upper limit, $\sqrt{3/5}$. This is highly unusual, yet a very recent paper reports a similar effect in a pNIPAM microgel with a hydrophobic crosslinker [20]; we speculate that in this case the effect may be due to competition between the hydrophobicity of the crosslinker and pNIPAM at high temperatures. Our results suggest another new path for generating microgels with high $R_g/R_h$ morphology.

Research conducted at ORNL's Spallation Neutron Source was sponsored by the Scientific User Facilities Division, Office of Basic Energy Sciences, US Department of Energy. Funding was provided by the ACS Petroleum Research Fund (50603-DNI7), the IBB seed grant program and Shinsegae International Co.

[1] X. Wu, R. Pelton, A. Hamielec, D. Woods, and W. McPhee, Colloid Polym. Sci. **272**, 467 (1994).
[2] M. Seeber, B. Zdyrko, R. Burtovvy, T. Andrukh, C.-C. Tsai, J. Owens, K. Kornev, and I. Luzinov, Soft Matter **7**, 9962 (2011).
[3] I. Varga, T. Gilányi, R. Mészáros, G. Filipcsei, and M. Zrínyi, J. Phys. Chem. B **105**, 9071 (2001).
[4] M. Stieger, W. Richtering, J. Pedersen, and P. Lindner, J. Chem. Phys. **120**, 6197 (2004).
[5] T. Hellweg, J. Polym. Sci. Part B Polym. Phys. **51**, 1073 (2013).
[6] K. Schätzel, J. Mod. Opt. **38**, 1849 (2007).
[7] J. Dhont, *An Introduction to Dynamics of Colloids*, 2nd ed. (Elsevier Science B.V., Amsterdam, 2003).
[8] B. Saunders, Langmuir **20**, 3925 (2004).
[9] M. Reufer, P. Díaz-Leyva, I. Lynch, and F. Scheffold, Eur. Phys. J. E **28**, 165 (2009).
[10] R. Chen, H. Yang, X. Yan, Z. Wang, and L. Li, Chem. J. Chin. U. **22**, 1262 (2001).
[11] *Acrylic Acid*, Base Acrylic Monomer Manufacturers, Inc. (2013), 4th Ed.
[12] A. Routh and W. Zimmerman, J. Colloid Interface Sci. **261**, 547 (2003).
[13] W. Dozier, J. Huang, and L. Fetters, Macromolecules **24**, 2810 (1991).
[14] P. Debye and A. Bueche, J. Appl. Phys. **20**, 518 (1949).
[15] J. Clara-Rahola, A. Fernandez-Nieves, B. Sierra-Martin, A. South, L. Lyon, J. Kohlbrecher, and A. Fernandez-Barbero, J. Chem. Phys. **136**, 214903 (2012).
[16] Z. Ahmed, E. Gooding, K. Pimenov, L. Wang, and S. Asher, J. Phys. Chem. B **113**, 4248 (2009).
[17] Y. Weng, Y. Ding, and G. Zhang, J. Phys. Chem. B **110**, 11813 (2006).
[18] M. Villarino, arXiv , 0511652v1 (2008).
[19] A. Fernández-Barbero, A. Fernández-Nieves, I. Grillo, and E. López-Cabarcos, Phys. Rev. E **66**, 051803 (2002).
[20] G. Deen and J. Pedersen, Cogent Chemistry **1**, 1012658 (2015).